Available online at www.sciencedirect.com

ScienceDirect

Procedia Structural Integrity 13 (2018) 1141–1147

Structural Integrity Procedia

www.elsevier.com/locate/procedia

ECF22 - Loading and Environmental effects on Structural Integrity

Features of the Hydrogen-Assisted Cracking Mechanism in the Low-Carbon Steel at Ex- and In-situ Hydrogen Charging

E.D. Merson[a], P.N. Myagkikh[a], V.A. Poluyanov[a], D.L. Merson[a], A. Vinogradov[b]

[a]*Institute of Advanced Technologies, Togliatti State University, Belorusskaya str. 14, Togliatti 445667, Russian Federation*

[b]*Department of Mechanical and Industrial Engineering, Norwegian University of Science and Technology – NTNU, N-7491 Trondheim, Norway*

Abstract

Hydrogen embrittlement has been intensively studied in the past. However, its governing mechanism is still under debate. Particularly, the details of the formation of specific cleavage-like or quasi-cleavage fracture surfaces related to hydrogen embrittled steels are unclear yet. Recently it has been found that the fracture surface of the hydrogen charged and tensile tested low-carbon steel exhibits quasi-cleavage facets having specific smoothly curved surface, which is completely different from common flat cleavage facets. In the present contribution we endeavor to shed light on the origin of such facets. For this purpose the notched flat specimens of the commercial low carbon steel were tensile tested using ex- and in-situ hydrogen charging. It is found that in the ex-situ hydrogen charged specimens the cracks originate primarily inside the specimen bulk and expand radially form the origin to the specimen surface. This process results in formation of "fisheyes" – the round-shape areas with the surface composed of curved quasi-cleavage facets. In contrast, during tensile testing with in-situ hydrogen charging, the cracks initiate from the surface and propagate to the bulk. This process results in the formation of the completely brittle fracture surface with the quasi-cleavage morphology - the same as that in fisheyes. The examination of the side surface of the in-situ hydrogen charged specimens revealed the straight and S-shaped sharp cracks which path is visually independent of the microstructure and crystallography but is strongly affected by the local stress fields. Nano-voids are readily found at the tips of these cracks. It is concluded that the growth of such cracks occurs by the nano-void coalescence mechanism and is responsible for the formation of fisheyes and smoothly curved quasi-cleavage facets in hydrogen charged low-carbon steel.

Peer-review under responsibility of the ECF22 organizers.

Keywords: hydrogen embrittlement; fracture surface; quasi-cleavage;

2452-3216
Peer-review under responsibility of the ECF22 organizers.
10.1016/j.prostr.2018.12.238

1. Introduction

Many steels and other alloys absorbing hydrogen suffer from substantial degradation of mechanical properties. In particular, the drop of ductility caused by hydrogen can result in a dramatic reduction of service life and sudden failures of metallic structures. This phenomenon commonly known as hydrogen embrittlement (HE) for years remains an essential problem for oil, gas, aerospace, nuclear energy and many other key industries. Although a lot of efforts have been made to find the rational ways of eliminating the harmful hydrogen influence, all the attempts are not fully successful because of still existing deficiency of understanding of the HE nature and the mechanisms governing the hydrogen-assisted cracking (HAC). Despite the vast number of publications in the field and the abundance of accumulated experimental data, some important aspects and details of HAC process are still missing or unclear. One of such open issues is the nature and the formation mechanism of the so-called quasi-cleavage (QC) fracture surfaces referred also to as "cleavage-like" or "quasi-brittle", which are found frequently in the bcc steels and iron embrittled by hydrogen Lynch (2012), Martin et al. (2011), Neeraj et al. (2012), Takahashi et. al. (2011) Takano et. al. (1993). There is strong belief that fracture surfaces of this kind are unique because they possess specific features distinguishing them from all other kinds of fracture surfaces including true cleavage and "original" QC that is found usually in martensitic steels Kikuta et al. (1978), Merson et al. (2016), Nakasato and Bernstein (1978). Using confocal laser scanning microscopy (CLSM) it was recently established that QC facets in the hydrogen embrittled low-carbon steel have a wavy-like curved profile even on the scale of a single grain while their average misorientation angle is twice as small as that of low-temperature cleavage facets in the same steel Merson et al. (2016). The curviness of the QC facets implies that a specific mechanism leads to their formation, and that this mechanism is different from normal brittle transgranular cracking that produces flat facets aligned with well-defined crystallographic planes. It was supposed that QC facets can be formed by a sort of microvoid coalescence (MVC) process modified by hydrogen Martin et al. (2011), Neeraj et al. (2012). If the HAC producing curved QC facets is accompanied by the void nucleation and coalescence, one should be able to observe this process on the side surface of the hydrogen embrittled specimen during the crack growth test. *Thus the main purpose of the present study was to clarify the origin of the curved QC facets in the hydrogen embrittled low-carbon steel by side surface microscopic observations.* Two different experimental approaches were implemented: (1) ex-situ hydrogen charging of the low-carbon steel specimens followed by tensile testing inside the scanning electron microscope (SEM) with in-situ observation of the damage development on the side surface, and (2) in-situ hydrogen charging during tensile testing outside of the SEM chamber followed by the post-mortem microscopic examination of the side surface.

2. Experimental

Using the electric-discharge machine, the flat rectangular specimens ($60\times11\times2$ mm^3) with a center through-notch have been cut from the hot-rolled plate of commercial low-carbon steel grade S235JR. The chemical composition of the steel is provided in Table 1. The specimens were grounded by emery paper number #2500 and then annealed in vacuum at 950 °C for 30 min. Finally, the one face of the specimens was additionally polished with 1 μm suspension followed by electro-polishing of the 2 cm^2 area around the notch.

Table 1. Chemical composition of the steel S235JR.

Element	C	Cu	Si	Mn	P	S	Cr	Ni	Al	Fe
Wt (%)	0.129	0.067	0.02	0.42	0.019	0.015	0.05	0.007	0.028	Balance

Ex-situ cathodic hydrogen charging of the specimens was held at 200 mA/cm^2 current density during 1 h. In-situ hydrogen charging was performed at 5 mA/cm^2 with the use of the electrochemical cell mounted on the middle part of the specimen during tensile testing. The platinum anode and the electrolyte containing 5% H_2SO_4 with addition of 1.5 g/l thiourea were used for the both types of hydrogen charging.

The uniaxial tensile test with simultaneous (in-situ) hydrogen charging was conducted at normal pressure and room temperature at 0.1 mm/min initial crosshead velocity using a screw-driven H50KT (Tinius Olsen) testing machine. No pre-charging was used in these tests. The ex-situ hydrogen charged (precharged) specimens were

tensile tested in air at normal pressure and room temperature as well as under vacuum inside the chamber of the SEM, SIGMA (Carl Zeiss). For tensile testing inside the SEM chamber, the Kammrath & Weiss micromechanical module was used. Time between the end of ex-situ hydrogen charging and the start of tensile test was about 10 and 30 minutes for the tests outside and inside SEM, respectively.

3. Results

3.1. Before hydrogen charging

The experiments inside the SEM chamber showed that, as generally accepted, the tensile test of the annealed low-carbon steel, which was not subjected to hydrogen charging, included several stages: (1) the elastic stage with no noticeable changes of the microstructure on the side surface of the specimen, Fig. 1a, b; (2) the yielding stage featured by the plateau region on the loading diagram and by the plastic zone formation around the notch, Fig. 1a, c; (3) the strain-hardening stage accompanied by the increasing load and the extending plastic zone, Fig. 1a, d; (4) nucleation of voids and micro cracks in the vicinity of the notch at the peak load, Fig. 1a, e-g, followed by (5) load decrease caused by the reduction of the cross-section area of the specimen due to propagation of the main crack from the notch to the opposite face of the specimen, Fig. 1a, h, i. As follows from Fig. 1e-g, the crack growth is accompanied by voids nucleation ahead of the crack and by intensive plastic deformation as is evidenced by numerous slip lines surrounding the crack tip. The fracture surface of the reference specimen exhibits a typical ductile dimpled appearance.

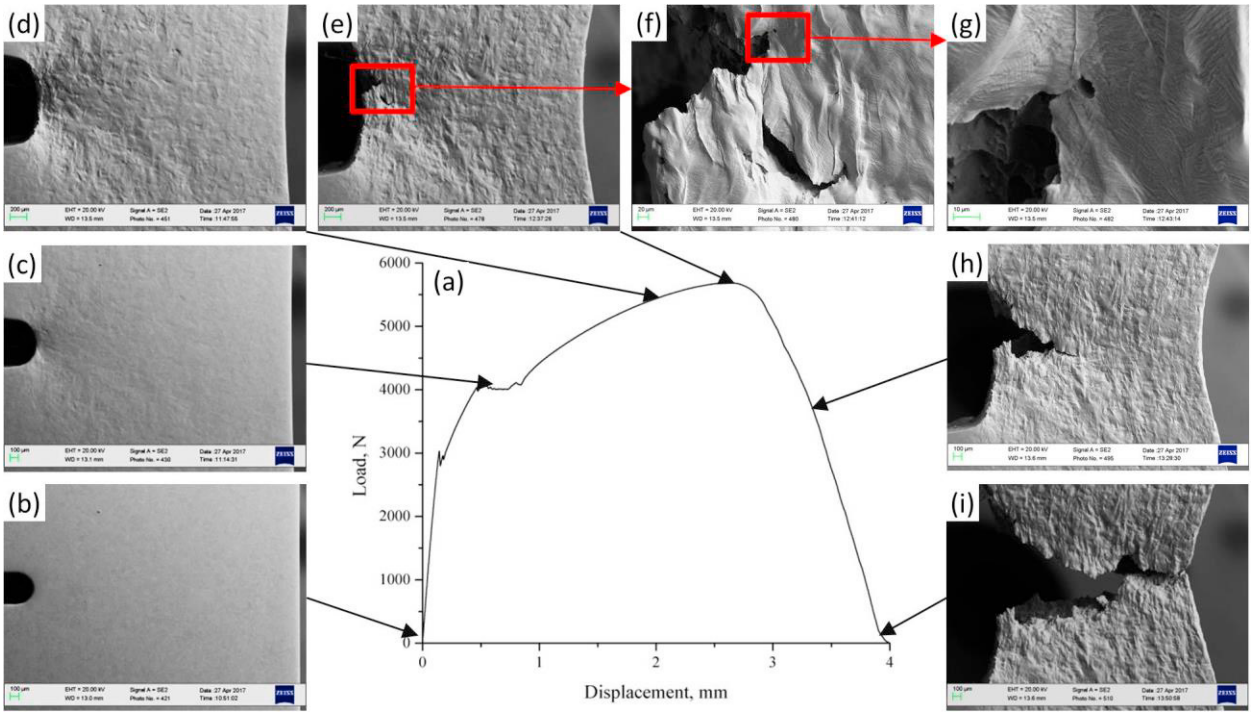

Fig. 1. Loading diagram (a) and the side surface SEM images (b-i) at different stages of the tensile test of the reference specimen.

3.2. Ex-situ hydrogen charging

After ex-situ hydrogen charging, the specimen's surface is covered with blisters and hydrogen-induced cracks (HICs), see Fig. 2b, c. The tensile tests in air as well as in vacuum showed that hydrogen charging eliminates the yield plateau on the loading diagram and results in the reduction of the maximum load and displacement before fracture, Fig. 2a. In comparison with the reference specimen, the extent of plastic deformation is very low even at

the end of strain-hardening stage featured by microvoids formation in the vicinity of the notch Fig. 2d, e. When the maximum stress is reached, several micro cracks opened at the notch as well as at some blisters and HICs as shown by arrows in Fig. 2f, g. The further growth and coalescence of these micro cracks leads to the final fracture, Fig. 2i, which occurs much faster than in the reference specimen. However, one can see at the higher magnification that the growth and coalescence of the micro cracks is accompanied by the formation of voids and slip lines, Fig. 2h, which resemble those observed during the ordinary ductile fracture of the not charged specimens.

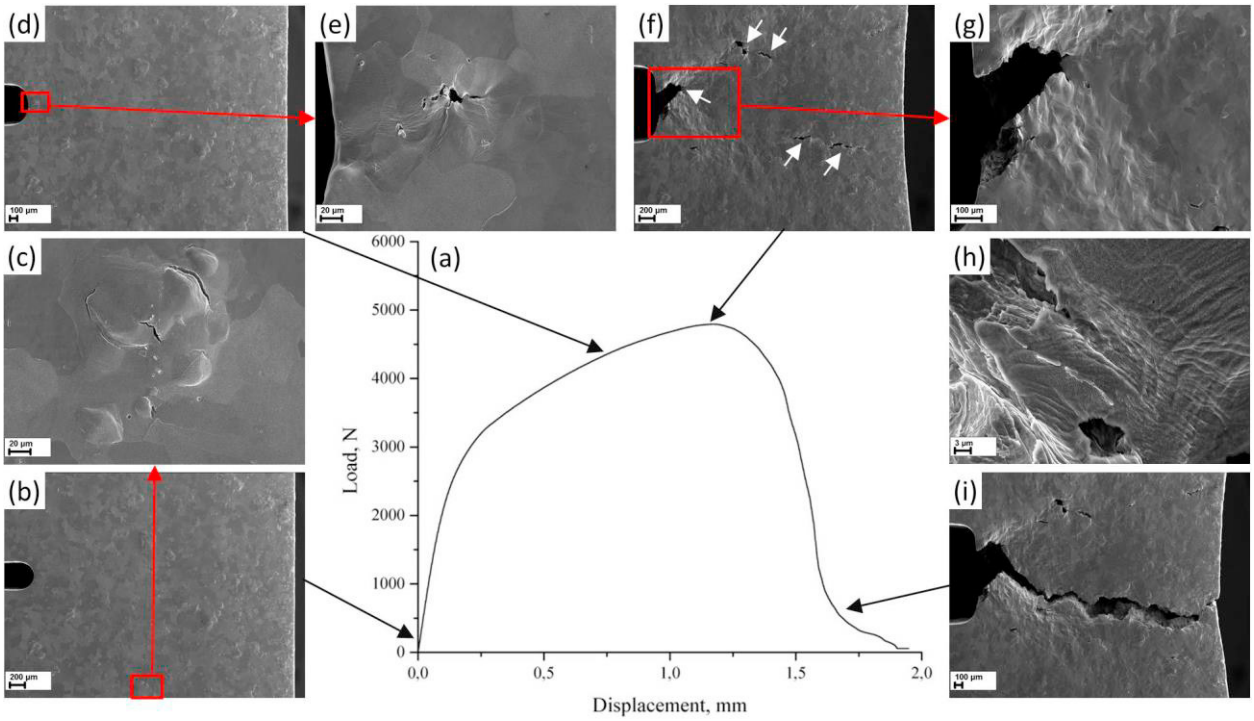

Fig. 2. Loading diagram (a) and the side surface SEM images (b-i) at different stages of the tensile test of the ex-situ hydrogen charged specimen.

As can be seen in Fig. 3a, b, the fracture surface of the hydrogen charged specimens contains round-shape brittle areas – the so called “fisheyes”. These defects are composed of QC facets which appearance is the same to the smoothly curved ones observed in our previous dedicated study E. Merson et al., 2016. The fracture surface around the fisheyes has a ductile dimpled relief. It is known that the formation of fisheyes occurs by the hydrogen-assisted growth of cracks in the normal to the tensile axis direction Merson et al. (2018). These cracks are initiated at non-metallic inclusions or at other regions of high hydrogen and stress concentration. As follows from the fractographic analysis in the present case, most of fisheyes were nucleated at cracks oriented perpendicular to the fracture surface and along the tensile axis, see Fig. 3b. Such cracks were not found in the microstructure and on the fracture surface of the reference specimens. Therefore, apparently these cracks are HICs, which were formed during hydrogen charging. Indeed HICs are known as hydrogen traps containing hydrogen inside their inner volume as well as in the ~50 μm layer around them Griesche et al. (2014). Taking into account that these cracks also serve as stress risers, the nucleation of fisheye cracks at HICs is well expected. As follows from the orientation of the river lines on the facets, the fisheyes extend radially from the initiation cites. When the thickness of the ligament between two fisheyes (or between the fisheye and the side surface of the specimen) becomes critically small, the necking followed by ductile rupture occurs. This process causes the formation of dimpled relief around QC areas. It is found that fisheyes almost never exit to the side surface of the specimen. Even when they approach very close to the side surface, the narrow streak of the dimpled relief always appears between the fisheye and the surface, Fig. 3c. Thereby most of ductile fracture features, which appeared on the side surface of the ex-situ hydrogen charged specimen

during the tensile test, Fig. 2e-h, cannot be directly attributed to HAC. This circumstance substantially complicates revealing the HAC mechanism during ex-situ hydrogen charging.

3.3. In-situ hydrogen charging

The fractographic examination showed that the fracture surface of the in-situ hydrogen charged specimen is completely brittle and is presented only by the QC morphology, Fig. 3d-f. The ductile dimpled relief is not found on the fracture surface including its near side surface regions. The appearance of the QC morphology is the same as that of fisheyes in the ex-situ hydrogen charged specimens, Fig. 3e, f. This observation suggest that the similar mechanisms of HAC operate during ex-situ and in-situ hydrogen charging. However, in the ex-situ charged steel HAC is strongly interfered with the MVC ductile fracture. As was shown above, the later can completely hinder the features of HAC on the side surface of the ex-situ charged steel because the cracks in this case grow internally from the bulk to the specimen's surface, and they almost never exit to the surface. In contrast, in-situ hydrogen charging persistently provides a high hydrogen concentration at the specimen's surface so that the cracks are promoted to originate at the surface and propagate into the bulk. This is well confirmed by the orientation of the river lines on the fracture surface of the in-situ charged specimen. Thus, the in-situ hydrogen charging is preferable for investigation of the HAC mechanism by the side surface microscopic analysis. Although the in-situ tensile testing inside SEM chamber with in-situ cathodic hydrogen charging is still challenging, even the post-mortem examination of the specimen's side surface renders useful information about HAC as will be demonstrated below.

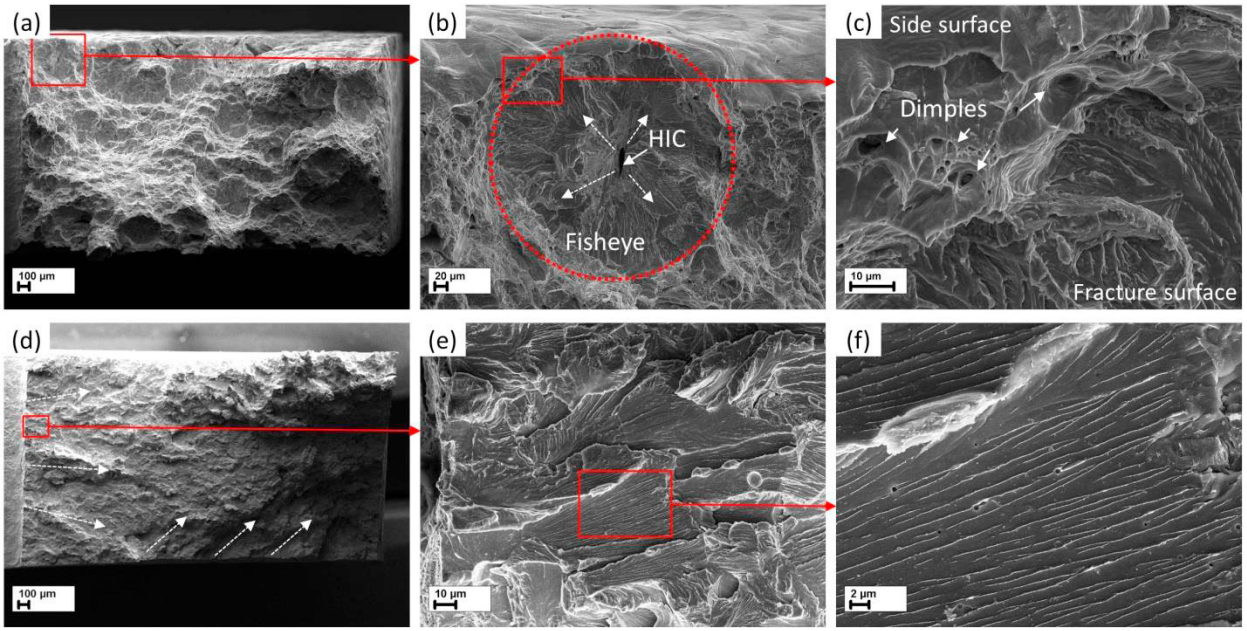

Fig. 3. Fracture surfaces of the ex-situ (a-c) and in-situ (d-f) hydrogen charged specimens: (a, d) – full view; (b) – "fisheye" defect nucleated at hydrogen-induced crack and extended in the radial direction from the nucleation point; (c) – streak of ductile dimpled fracture surface between quasi-cleavage relief of the fisheye and side surface of the specimen; (e, f) - quasi-cleavage morphology at different magnifications. Dashed arrows in (b, d) indicate crack growth direction.

It is found that the side surface of the specimen tested during in-situ hydrogen charging contains numerous cracks but no blisters, Fig. 4. All cracks are observed only within the plastic zone beneath the fracture surface, Fig. 4a. Most of them have similar orientation, which is approximately normal to the tensile axis of the specimen. The observed cracks can be divided into two types. The cracks of the first are smoothly curved to the S-shape, and are found primarily in the area close to the notch, Fig. 4b, c. The shape of these cracks is exactly the same as the smoothly curved profiles of the QC facets, which were found in the same steel and documented in our previous study (see Fig. 8d in Merson et al. (2016)). The cracks of the second type are found farer from the notch and the

fracture surface, Fig. 4 d, e. These cracks are straighter albeit at higher magnification they also exhibit a pronounced waviness. The QC regions having the similar profile were also considered in the above-cited paper (see Fig. 8b in Merson et al. (2016)). Based on the results of fractographic analysis performed with the use of CLSM, it was concluded that the influence of crystallographic orientation of grains on the QC fisheye crack path is less important in comparison with brittle cleavage cracking. The appearance of the cracks observed in the present study on the side surface of the in-situ hydrogen charged specimen strongly corroborates this conclusion. As can be seen in Fig. 4e, the cracks can cross the grain boundaries without deviation of their growth direction. This appears to be in contrast, for example, with the cleavage cracks, which tend to align themselves with {001} crystallographic planes in each grain Burghard and Stoloff (1968). Moreover, these cracks can smoothly change their growth direction within a single grain, Fig. 4c. Thus taking into account the relationship between the shape of the cracks and their position with respect to the notch and to each other, we can conclude that the interaction of the stress fields of the notch and the cracks is the much more important factor determining the path and the behavior of the quasi-cleavage cracks in the hydrogen-embrittled low-carbon steel than the microstructural details and the crystallographic orientation of individual grains in this steel.

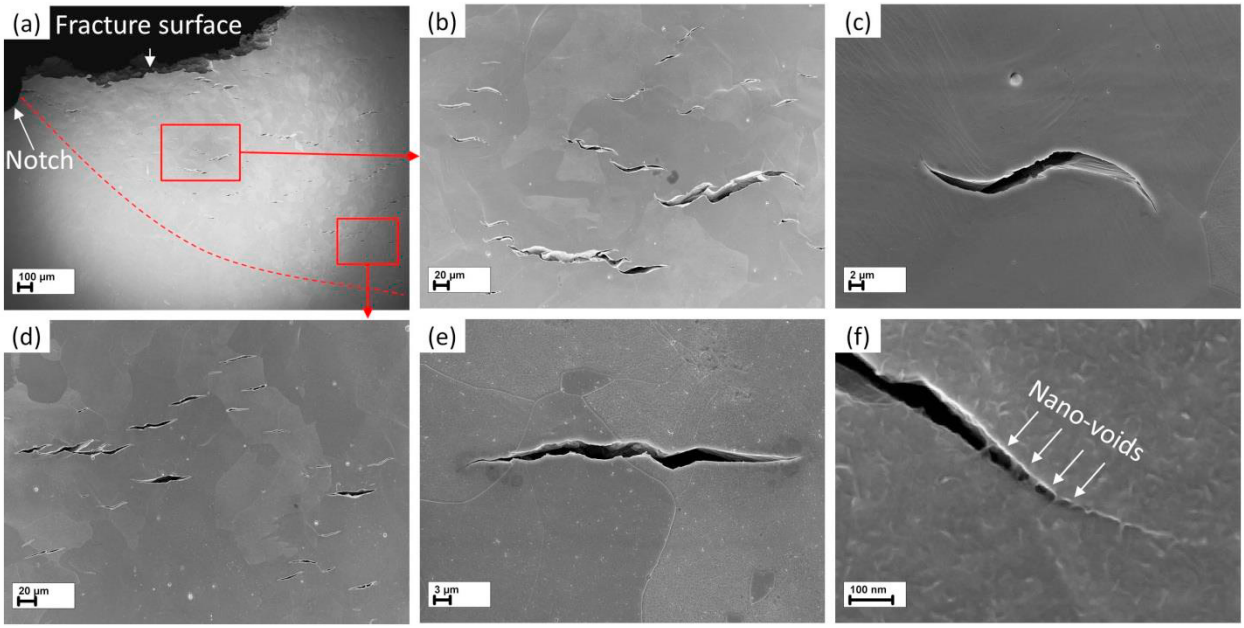

Fig. 4. Side surface of the in-situ hydrogen charged specimen exhibiting S-shape (b, c) and straighter (d, e) cracks. Dashed line on the (a) indicates boundary of the plastic zone ahead of the notch.

Such a behavior of the cracks can be explained if one assumes that the crack growth occurs by the microvoid coalescence process. It can be seen in Fig. 4c, e that the cracks in the in-situ hydrogen charged specimen are much sharper in comparison with the blunted cracks observed on the side surface of the ex-situ hydrogen charged specimens, c.f. Fig. 2g, h. It is clear that hydrogen supplied to the specimen's surface during in-situ charging prevents blunting of the cracks so they stay sharp. At first glance, they are completely brittle. Despite the presence of the slip lines occasionally emanating from the cracks or crossing them, no large voids ahead of the cracks' tips, such as those in Fig. 2e and h, are found. However, at the sufficiently high magnification it is obvious that the crack tip region contains nano-voids of 10-50 nm size as illustrated in Fig. 4f. These voids coalesce by ductile rupture of thin ligaments between them, producing cups-like profile of the crack surface. Thus, the growth of these cracks is the ductile process by nature. This conclusion is in good agreement with hydrogen-enhanced localized-plasticity (HELP) and adsorption-induced dislocation emission (AIDE) models Lynch et al. (2012), which predict that hydrogen should facilitate and localize dislocation processes resulting in enhancement of the crack growth by a dislocation-mediated microscopically ductile mechanism.

4. Conclusions

1. The propagation of the cracks resulting in formation of fisheye defects and smoothly curved quasi-cleavage facets on the fracture surface of the hydrogen embrittled low-carbon steel occurs by the nano-void calescence process.
2. The main factor determining the propagation path of these cracks is the stress distribution while the influence of the microstructure as well as the crystallographic orientation of grains is less significant even on the scale of a single grain.
3. Hydrogen prevents plastic blunting of these cracks, provided that its concentration at cracks tips is high enough.
4. In the case of ex-situ hydrogen charging, hydrogen-assisted cracking occurs mainly in the bulk of the specimen by the formation of fisheye defects while the fracture of the specimens surface occurs primarily by the microvoid coalescence process causing the familiar ductile dimpled fracture. In-situ hydrogen charging maintains high concentration of hydrogen at the specimen's surface so the cracks originate at the surface and propagate into the bulk producing completely brittle quasi-cleavage fracture surface without ductile regions featured by large dimples.

Acknowledgments

Financial support from the Russian Foundation for Basic Research (grant-in-aid 17-08-01033) is gratefully acknowledged.

References

Burghard, H. C., Stoloff, N. S. (1968). Cleavage Phenomena and Topographic Features. In: "Electron Fractography". In: C. D. Beachem (Ed.), pp. 32–58.

Griesche, A., Dabah, E., Kannengiesser, T., Kardjilov, N., Hilger, A., Manke, I. (2014). Three-dimensional imaging of hydrogen blister in iron with neutron tomography. Acta Materialia, 78, 14–22.

Kikuta, Y., Araki, T., & Kuroda, T. (1978). Analysis of Fracture Morphology of Hydrogen-Assisted Cracking in Steel and Its Welds. In: "Fractography in Failure Analysis". In B. M. Strauss, W. H. Cullen (Eds.), pp. 107–127.

Lynch, S. P. (2012). Hydrogen embrittlement phenomena and mechanisms. Corrosion Reviews, 30 (3–4), 63–133.

Martin, M. L., Fenske, J. A., Liu, G. S., Sofronis, P., & Robertson, I. M. (2011). On the formation and nature of quasi-cleavage fracture surfaces in hydrogen embrittled steels. Acta Materialia, 59(4), 1601–1606.

Merson, E. D., Myagkikh, P. N., Klevtsov, G. V., Merson, D. L., & Vinogradov, A. (2018). Effect of fracture mode on acoustic emission behavior in the hydrogen embrittled low-alloy steel. Engineering Fracture Mechanics, (January).

Merson, E., Kudrya, A. V., Trachenko, V. A., Merson, D., Danilov, V., & Vinogradov, A. (2016). Quantitative characterization of cleavage and hydrogen-assisted quasi-cleavage fracture surfaces with the use of confocal laser scanning microscopy. Materials Science and Engineering: A, 665, 35–46.

Nakasato, F., & Bernstein, I. (1978). Crystallographic and fractographic studies of hydrogen- induced cracking in purified iron and iron- silicon alloys. Metallurgical and Materials Transactions A, 9(9), 1317–1326.

Neeraj, T., Srinivasan, R., & Li, J. (2012). Hydrogen embrittlement of ferritic steels: Observations on deformation microstructure, nanoscale dimples and failure by nanovoiding. Acta Materialia, 60(13–14), 5160–5171.

Takahashi, Y., Yamaguchi, K., Tanaka, M., Higashida, K., & Noguchi, H. (2011). On the micromechanism of hydrogen-assisted cracking in a single-crystalline iron-silicon alloy thin sheet. Scripta Materialia, 64(6), 537–540.

Takano, N., Kidani, K., Hattori, Y., & Terasaki, F. (1993). Fracture surface of hydrogen embrittlement in iron single crystals. Scripta Metallurgica et Materialia, 29(1), 75–80.